Confinement and amplification of acoustic waves in cubic heterostructures

S. M. Komirenko and K. W. Kim
Department of Electrical and Computer Engineering, North Carolina State University, Raleigh, North Carolina 27695-7911

V. A. Kochelap
Department of Theoretical Physics, Institute of Semiconductor Physics, National Academy of Sciences of Ukraine, Kiev-28, 252650, Ukraine

M. A. Stroscio
Department of Electrical and Computer Engineering, University of Illinois, Chicago, Illinois 60607-7052
(Received 17 April 2001; published 4 April 2002)

We present the theory of acoustic phonon confinement in elastically anisotropic (cubic) quantum-well (QW) heterostructures grown in a direction of high symmetry. A general criterion for phonon confinement is derived. For $Si/Si_{0.5}Ge_{0.5}/Si$, Si/Ge/Si and AlAs/GaAs/AlAs QW heterostructures, dispersion curves are obtained, and displacement fields corresponding to the confined phonons are studied in detail. It is found that the confinement of acoustic phonons in these QW layers is strong in the subterahertz and terahertz frequency ranges. The resulting description of phonon confinement is applied to analyze the amplification of confined modes by the drift of the two-dimensional carriers as a function of the phonon frequency, the temperature, and the parameters of heterostructure. The calculation shows that the amplification coefficient of the confined phonons can exceed 10^3 cm^{-1} for Si/Ge-based structures and 10^2 cm^{-1} for AlAs/GaAs-based structures.

DOI: 10.1103/PhysRevB.65.155321 PACS number(s): 72.20.−i, 68.65.−k, 63.20.Kr, 63.22.+m

I. INTRODUCTION

The layered character of semiconductor heterostructures causes the acoustic vibrations of the lattice to be different from the usual bulklike waves. This difference manifests itself in surface[1] and leaky surface[2] waves, interface[3] and leaky interface[4] waves, confined waves in quantum well heterostructures,[5–7] and folded acoustic phonons in superlattices.[8,9] Interacting with two-dimensional electrons, the modified lattice vibrations contribute to kinetic phenomena and different acoustoelectric effects. For example, the surface and confined waves determine the low-temperature electron mobility in perfect heterostructures,[6,10–12] and the leaky interface waves are responsible for the magnetophonon resonance.[13] The surface waves were employed to control the electric current (including single-electron transport) in quantum wells and wires.[14,15] In general, a number of applications of acoustic waves in layered quantum heterostructures can be realized to control electron transport, to modulate electric currents and optical signals, and to enhance overall device performance.

Since the methods of generation and detection of the surface waves are well developed, these waves and their interaction with electrons have been studied the most extensively. Nevertheless, the confined acoustic waves in quantum-well (QW) structures can be of great importance for high-frequency effects and various applications. Indeed, the confinement of acoustic modes increases progressively with frequency. This can result in a strong phonon coupling to low-dimensional electrons in a high-frequency range. Recently, it was suggested that the confined high-frequency phonons can be amplified by the drift of two-dimensional electrons.[16] A realization of this effect in semiconductor heterostructures would open up interesting perspectives for the generation of coherent high-frequency confined phonons and for the study of confined electron–confined phonon interaction.

Confinement of the acoustic phonons is possible due to the mismatch in elastic properties of layers composing QW heterostructures. Typically, this mismatch is small, and confinement properties are sensitive to both the mismatch and symmetry of crystals composing the heterostructure. (A general analysis of possible acoustical waves in layered systems can be found in Refs. 17–19.) Previously, confined waves[5] and their amplification[16] were studied based on a simple model of *elastically isotropic* media. In this paper, we develop a model of *elastically anisotropic (cubic)* media for layers constituting the heterostructure to make an analysis of the confined modes and their amplification (generation) more realistic.

The rest of the paper is organized as follows. In Sec. II, we formulate the basic equations and present an analysis of the confined phonons in cubic QW heterostructures grown in the [001] direction. In Sec. III, we apply this analysis to Si/Ge/Si, $Si/Si_{0.5}Ge_{0.5}/Si$, and AlAs/GaAs/AlAs QW's, considering the confined vibrations in details. In Sec. IV, the theory is extended to the problem of confined phonon amplification. A summary follows in Sec. V. Some of the detailed formulas are collected in Appendixes A and B.

II. CONFINEMENT OF ACOUSTIC MODES IN CUBIC HETEROSTRUCTURES

Consider the heterostructure shown in Fig. 1, where electrons are confined in a QW layer A embedded in a semiconductor material B. The thickness of layer A is $2d$. Both materials A and B are supposed to be of cubic symmetry. We assume that the structure is grown in the [001] direction, and that the propagation direction of the acoustic wave is [100].

 ©2002 The American Physical Society

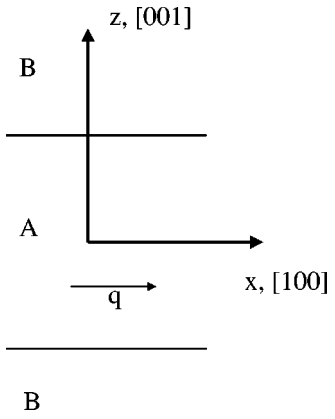

FIG. 1. Geometry of the heterostructure under analysis.

Within the framework of the linear theory of elasticity, acoustic vibrations in each of the media can be described by the equation of motion[20]

$$\rho \frac{\partial^2 u_i}{\partial t^2} = \frac{\partial \sigma_{ij}}{\partial x_j}, \quad x_i = x,y,z, \tag{1}$$

where ρ is the mass density, u_i are the components of the displacement vector, x, y, and z are the coordinates, and σ_{ij} are the components of the stress tensor. Applying Hooke's law for a cubic crystal, the stress tensor can be written as

$$\sigma_{ij} = C_{12}(div\ \mathbf{u})\delta_{ij} + C_{44}\left(\frac{\partial u_i}{\partial x_j} + \frac{\partial u_j}{\partial x_i}\right) + D\frac{\partial u_i}{\partial x_j}\delta_{ij}, \tag{2}$$

where

$$D = C_{11} - C_{12} - 2C_{44} \tag{3}$$

is the parameter of anisotropy and the summation over i and j is not assumed in the last term of Eq. (2).

For elastically isotropic media, $D=0$. In general, $D\neq 0$, which results in the anisotropy of the propagation of the acoustic waves. For long-wavelength acoustic waves, the dispersion relations between the frequency ω and the wave vector $\mathbf{q}$ become dependent on the wave-vector orientation: $\omega = V(\mathbf{q})q$, where $\mathbf{V}(\mathbf{q})$ is the wave velocity. In particular, Eqs. (1)–(3) imply that if the wave vector is on the (010) plane [i.e., if $\mathbf{q}=(q\sin\theta,0,q\cos\theta)$], there are three types of the waves: quasilongitudinal and quasitransverse waves with orientation-dependent velocities,

$$V_{L,T}^{(quasi)}(\theta) = \sqrt{[(C_{11}+C_{44}) \pm \sqrt{(C_{11}-C_{44})^2 - \sin^2(2\theta)D(C_{11}+C_{12})}]/2\rho}, \tag{4}$$

and a purely transverse wave with a velocity

$$V_T = \sqrt{C_{44}/\rho}. \tag{5}$$

The upper sign in Eq. (4) corresponds to the quasilongitudinal waves which comprise both longitudinal and transverse lattice vibrations. For [100] and [101] high-symmetry directions, the quasilongitudinal waves reduce to purely longitudinal ones with velocities $V_L^{(quasi)}(0) = V_L^{[100]} = \sqrt{C_{11}/\rho}, V_L^{(quasi)}(\pi/4) = V_L^{[101]} = \sqrt{(C_{11}-D/2)/\rho}$, respectively. For arbitrary θ the dispersion curves $\omega(\mathbf{q})$ fall into the sector S_L determined by the lines $\omega = V_L^{[100]}q$ and $\omega = V_L^{[101]}q$ in the (ω,q) plane. Analogously, the quasitransverse waves [the lower sign in Eq. (4)] comprising, in general, transverse and longitudinal vibrations, become purely transverse for the high-symmetry directions with velocities $V_T^{(quasi)}(0) = V_T^{[100]} = \sqrt{C_{44}/\rho}, V_T^{(quasi)}(\pi/4) = V_T^{[101]} = \sqrt{(C_{44}+D/2)/\rho}$. In the (ω,q) plane their dispersion curves fall into the sector S_T limited by the lines $\omega = V_T^{[101]}q$ and $\omega = V_T^{[100]}q$. Obviously, the sector S_L is always above the sector S_T in the (ω,q) plane. Acoustic waves propagate in a bulk material only when they have values of ω and q which fall into sectors S_L or S_T.

For the geometry given in Fig. 1, Eqs. (1)–(3) should be supplemented by the boundary conditions at the interfaces:

$$u_i^A = u_i^B, \quad \sigma_{iz}^A = \sigma_{iz}^B \ \text{ at } \ z = \pm d. \tag{6}$$

Throughout this paper, the indices A and B label the materials. According to the definition, confined waves propagate along the A layer and decay outside it. The latter requirement provides additional boundary condition: $\mathbf{u}^B \to 0$ at $z = \pm\infty$. Two classes of the confined acoustic waves, shear-horizontal (SH) and shear-vertical (SV), can exist for the structures under consideration. The SH waves are purely transverse and polarized along the layer. The displacement vector for SH waves is $\mathbf{u}=(0,u_y,0)$. The shear-vertical waves (sagitally polarized waves) have two projections of the displacement vector: $\mathbf{u}=(u_x,0,u_z)$.

In the high-frequency region of interest, the dominant mechanism of electron–acoustic-phonon interaction is the interaction via the deformation potential. For this case, two-dimensional electrons with an isotropic energy dispersion are coupled only with *longitudinal* lattice vibrations. Thus we concentrate on an analysis of confinement of SV waves which comprise both longitudinal and transverse vibrations.

For SV waves, the components of the displacement vector can be represented as

$$u_x(x,z,t) = w_x(z)e^{i(qx-\omega t)},$$

$$u_z(x,z,t) = iw_z(z)e^{i(qx-\omega t)}. \tag{7}$$

One can show that functions $w_x(z)$ and $w_z(z)$ always have *different* symmetries. We define the symmetric shear-vertical (SSV) modes as those with $w_x(z) = w_x(-z), w_z(z) = -w_z$

$(-z)$ and the antisymmetric shear-vertical (ASV) modes as those with $w_x(z)=-w_x(-z), w_z(z)=w_z(-z)$.

The location of the sectors S_L and S_T in the (ω,q) plane is critically important for acoustic-phonon confinement. Since SV wave confined in the A layer comprises both longitudinal and transverse vibrations, solutions of the dispersion relation for such a wave have to be situated inside or between the sectors S_T^A and S_L^A. Then the confinement of a phonon with frequency ω_0 and two-dimensional wave vector q_0 is possible only if in the surrounding medium B there are no vibrations of the same frequency ω_0 and wave vector $\mathbf{q}=(q_0,0,q_z)$ with any arbitrary q_z. Otherwise, the vibrations excited in the QW layer will leak out. This implies that solutions of the dispersion relation of the confined SV waves cannot be found above the sector S_T^B. Thus the necessary condition of the confinement of the SV waves is the requirement for the sector S_T^A to be situated below the sector S_T^B, at least in part.

For the quantitative analysis of the confined waves, Eq. (1) provides the coupled equations for w_x and w_z in each medium,

$$w_x K_L^2(\omega,q)+\frac{d^2 w_x}{dz^2}C_{44}-q\frac{dw_z}{dz}[C_{11}-C_{44}-D]=0, \quad (8)$$

$$w_z K_T^2(\omega,q)+\frac{d^2 w_z}{dz^2}C_{11}+q\frac{dw_x}{dz}[C_{11}-C_{44}-D]=0, \quad (9)$$

where $K_L^2(\omega,q)=[\rho\omega^2-q^2C_{11}]$ and $K_T^2(\omega,q)=[\rho\omega^2-q^2C_{44}]$. The relations $K_L(\omega,q)=0, K_T(\omega,q)=0$ determine the dispersions of the bulk waves propagating in the [100] direction. A general solution to Eqs. (8) and (9) can be represented in the forms

$$w_x(z)=H_0 e^{\mathcal{R}_- z}+H_1 e^{-\mathcal{R}_- z}+H_2 e^{\mathcal{R}_+ z}+H_3 e^{-\mathcal{R}_+ z}, \quad (10)$$

$$w_z(z)=F_0^- e^{\mathcal{R}_- z}+F_1^- e^{-\mathcal{R}_- z}+F_2^+ e^{\mathcal{R}_+ z}+F_3^+ e^{-\mathcal{R}_+ z}, \quad (11)$$

with the following relationships between the coefficients:

$$F_j^{\mp}=(-1)^j\frac{q[C_{11}-C_{44}-D]\mathcal{R}_{\mp}}{K_T^2+C_{11}\mathcal{R}_{\mp}^2}H_j\equiv G_j^{\mp}(\omega,q)H_j.$$

Four exponential factors $\pm\mathcal{R}_{\mp}$ can be expressed in terms of ω and q as solutions to the biquadratic equation:

$$C_{11}C_{44}\mathcal{R}^4+\mathcal{R}^2[C_{11}K_L^2(\omega,q)+C_{44}K_T^2(\omega,q)+q^2(C_{11}-C_{44}-D)^2]+K_L^2(\omega,q)K_T^2(\omega,q)=0. \quad (12)$$

A general solution given by Eqs. (10) and (11) contains eight arbitrary constants H_j^M with $M=A,B$ and $j=0,1,2,3$; the solutions corresponding to the confined SSV and ASV waves have only four constants due to the symmetry requirements: $H_0^M=H_1^M$, $H_2^M=H_3^M$. For example, the SSV waves can be represented as

$$w_x(z)=\begin{cases} H_0^B\exp[\mathcal{R}_-^B z]+H_2^B\exp[\mathcal{R}_+^B z], \\ z<-d \\ H_0^A\cosh[\mathcal{R}_-^A z]+H_2^A\cosh[\mathcal{R}_+^A z], \\ |z|<d \\ H_0^B\exp[-\mathcal{R}_-^B z]+H_2^B\exp[-\mathcal{R}_+^B z], \\ z>d, \end{cases} \quad (13)$$

$$w_z(z)=\begin{cases} G_0^{-,B}H_0^B\exp[\mathcal{R}_-^B z]+G_2^{+,B}H_2^B\exp[\mathcal{R}_+^B z], \\ z<-d \\ G_0^{-,A}H_0^A\sinh[\mathcal{R}_-^A z]+G_2^{+,A}H_2^A\sinh[\mathcal{R}_+^A z], \\ |z|<d \\ -G_0^{-,B}H_0^B\exp[-\mathcal{R}_-^B z]-G_2^{+,B}H_2^B\exp[-\mathcal{R}_+^B z], \\ z>d, \end{cases} \quad (14)$$

with

$$\mathrm{Re}[\mathcal{R}_-^B(\omega,q)], \quad \mathrm{Re}[\mathcal{R}_+^B(\omega,q)]>0. \quad (15)$$

The ASV solutions can be obtained from Eqs. (13) and (14) by substituting sinh→cosh, cosh→sinh, and $H_{0,2}^B\to -H_{0,2}^B$ in the formulas for $z>d$.

For the SSV and ASV waves, boundary conditions (6) provide two systems of four linear homogeneous algebraic equations for the coefficient $H_{0,2}^{A,B}$. Characteristic matrices of these systems $\mathcal{D}^{SSV,ASV}$ are presented in Appendix A. Under criteria (15), the resolvability condition for these equations,

$$det|\mathcal{D}^{SSV,ASV}(\omega,q)|=0, \quad (16)$$

provides the dispersion relations for the confined SV waves.

In general, there is a *set* of solutions describing the confined waves with the dispersion relations $\omega_\nu(q)$, where ν is an integer. The solutions are orthogonal. Let us normalize the solutions by imposing the condition that the energy of the $\{\nu,q\}$ wave is equal to $\hbar\omega_\nu(q)$. According to the virial theorem, the kinetic energy of vibrations is equal to the potential (elastic) energy. The density of the elastic energy is $U_{el}^M=\frac{1}{2}\sigma_{ij}^M u_{ij}$, where u_{ij} are the components of the strain tensor. Thus, to normalize a solution $\mathbf{u}_{\nu q}$ properly, we use the condition[24]

$$2L_x L_y\int_{-\infty}^{\infty}dz\,\overline{U_{el}(z)}=\hbar\omega_{\nu q}, \quad (17)$$

where L_x and L_y are the lateral dimensions of the QW layer, and the bar shows the averaging over one period of the oscillations. In terms of the variables w_x and w_z, the elastic energy density is

$$\overline{U_{el}(z)}=\frac{1}{4}C_{11}\left[q^2w_z^2+\left(\frac{dw_z}{dz}\right)^2\right]+\frac{1}{4}C_{44}\left(\frac{dw_x}{dz}-qw_x\right)^2+\frac{1}{2}C_{12}qw_x\frac{dw_z}{dz}. \quad (18)$$

A normalization of the solutions (modes) given by Eq. (7) allows one to quantize the lattice vibrations and introduce *confined SV phonons*.

Prior to numerically calculating the SV solutions and the dispersion relations, we shall briefly discuss the exponential factors $\mathcal{R}_{\mp}$ which determine the acoustic confinement. It is convenient to present the solutions of Eq. (12) in each medium in the form

$$\mathcal{R}_{\mp}^{2}(\omega,q)=q^{2}R_{\mp}^{2}\left[\frac{\omega^{2}}{q^{2}}\right], \tag{19}$$

with

$$R_{\mp}^{2}\left[\frac{\omega^{2}}{q^{2}}\right]=\frac{\rho}{C_{44}}\frac{C_{11}+C_{44}}{2C_{11}}\left[\left(V_{0}^{2}-\frac{\omega^{2}}{q^{2}}\right)\mp\frac{C_{11}-C_{44}}{C_{11}+C_{44}}\sqrt{\left(\frac{\omega^{2}}{q^{2}}-V_{-}^{2}\right)\left(\frac{\omega^{2}}{q^{2}}+V_{+}^{2}\right)}\right]. \tag{20}$$

Here both quantities ω and q are real. The analytical expressions for the parameters V_0, V_-, and V_+ are given in Appendix B. When applied to an acoustic wave with the frequency ω and wave vector q, Eq. (20) represents the $R_{\pm}$ factors as functions of the phase velocity of this wave. The character of the $R_{\pm}$ factors changes at the $\omega/q=\text{const}$ lines and the solutions can be classified in the different sectors of the (ω,q)-plane.

The factors $R_{\mp}^{2}[\omega^{2}/q^{2}]$ are parametric functions of the anisotropy parameter D. We have studied $R_{\pm}$ at different D and found the following properties. For $D<0$, all parameters V_0, V_-, and V_+ are positive defined. In this case, Eq. (20) explicitly shows that $\mathrm{Re}[R_{\mp}]\neq 0$, $\mathrm{Im}[R_{\mp}]\neq 0$ for $\omega/q<V_-$. Solutions $\mathrm{Re}[R_{\pm}]=0$ and $\mathrm{Im}[R_{\pm}]\neq 0$ exist for $\omega/q>V_-$ if

$$D\leqslant D^{*}\equiv-[\sqrt{C_{11}(C_{11}-C_{44})}-(C_{11}-C_{44})], \tag{21}$$

and for $\omega/q>V_T$ otherwise. Thus the critical line, at which the factors $R_{\pm}$ change their character can be defined as $\omega=V_c q$ with

$$V_c=\begin{cases}V_- & \text{for } D\leqslant D^{*}\\ V_T & \text{otherwise.}\end{cases} \tag{22}$$

Let us apply this analysis to the confined phonons. First consider the surrounding medium where $\mathcal{R}_{\mp}^{B}(\omega,q)$ determine the decay of the waves. It is obvious that, in the B material, *leaky waves* appear only above the critical line. At and below this line confined modes can exist. Thus the line $\omega=qV_c^B$ is the *onset* for the dispersion of confined acoustic-phonon branches.

In the embedded material A, the critical velocity determines the asymptotical behavior of the dispersion branches for confined acoustic modes at $q\to\infty$. Indeed, in the limit $qd\gg 1$, a (ω,q) wave confined inside the QW layer can be considered as a superposition of bulklike plane waves with the wave vectors $(q,0,\pm q_z)$, where $q_z=|\mathcal{R}_{\pm}^{A}(\omega,q)|$ for purely imaginary $\mathcal{R}$ factors. Such factors exist only for $\omega>qV_c^A$.

TABLE I. Material parameters: mass densities (g/cm^3), stiffness constants and factors of anisotropy (10^{11} dyn/cm^2) and characteristic velocities (10^5 cm/sec).

Material	ρ	C_{11}	C_{44}	C_{12}	D	D^*	V_c
Si[a]	2.33	16.6	7.96	6.39	−5.71	−3.36	5.66
Ge[a]	5.33	12.85	6.80	4.83	−5.58	−2.77	3.37
$Si_{0.5}Ge_{0.5}$[b]	3.82	14.73	7.38	5.61	−5.65	−3.06	4.20
AlAs[c]	3.76	12.02	5.99	5.70	−5.66	−2.48	3.63
GaAs[c]	5.32	11.88	5.94	5.38	−5.38	−2.46	3.08

[a]Reference 21.
[b]Reference 22.
[c]Reference 23.

This analysis leads to the following conclusion: all confined acoustic branches have phase velocities which obey the relation

$$qV_c^A<\omega\leqslant qV_c^B. \tag{23}$$

It is important to emphasize that the condition given by Eq. (21) is typical for most of the semiconductor heterostructures, including the SiGe- and $Al_xGa_{1-x}As$-based structures considered in this paper. Consequently, for all these structures $V_c^M\equiv V_-^M$.

III. CONFINED PHONONS IN SiGe- AND $Al_xGa_{1-x}As$-BASED HETEROSTRUCTURES

In this section, we apply the results obtained previously in this paper to Si/Ge/Si, $Si/Si_{0.5}Ge_{0.5}/Si$, and AlAs/GaAs/AlAs QW heterostructures. Parameters used in the calculations, as well as the associated characteristic velocities are collected in Table I. From the data of Table I, it follows that for all these heterostructures as well as for the $Si_{0.5}Ge_{0.5}/Ge/Si_{0.5}Ge_{0.5}$ QW, condition (21) is valid and condition (23) can be satisfied. Thus, these structures are favorable for confinement of the SV phonons.[25]

First consider the SiGe heterostructures. For the Si/Ge/Si QW structure, in Fig. 2 we depict the sectors S_T^B and S_T^A, the onset line and an asymptote which corresponds to Eq. (23), and four lowest confined phonon branches. We use the dimensionless representation

$$\Omega=\frac{\omega}{\omega_0}\equiv\frac{\omega d}{V_T^A},\quad Q=qd.$$

In terms of these dimensionless quantities, the dispersion relations do not depend on the half-thickness of the layer d. Figure 2 clearly illustrates nearly all main features of the confinement of SV waves in the systems considered. For this case, the sectors S_T^B and S_T^A do not overlap. Equation (16) gives two sets of the dispersion curves which correspond to SSV and ASV solutions. For all structures, the lowest long-wavelength branch is found to be the lowest-order ASV

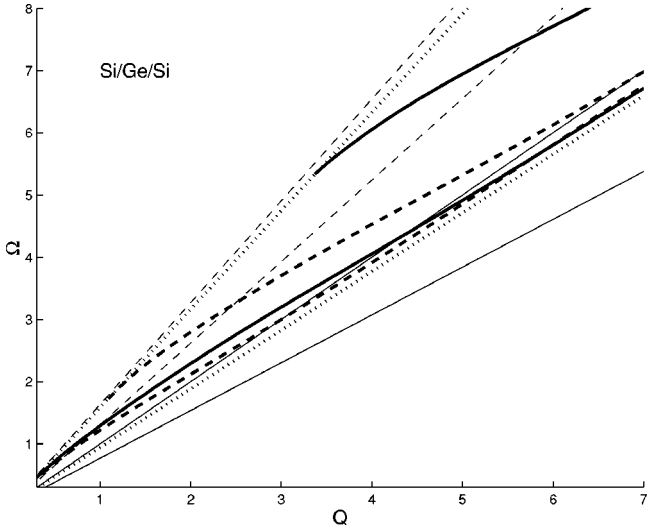

FIG. 2. Dispersion for Si/Ge/Si QW heterostructure. Sector S_T^B is delimited by thin dashed lines: the upper line has a slope $V_T^{[100],B}$, and the lower line has a slope $V_T^{[101],B}$. Sector S_T^A is delimited by thin solid lines: the upper line has a slope $V_T^{[100],A}$, and the lower line has a slope $V_T^{[101],A}$. In each sector S_T^M, the line with slope V_c^M is shown as the dotted line. Dispersions of the lowest two SSV (ASV) confined phonon branches are shown by the thick solid (dashed) lines.

branch which is denoted by ASV-0. At $Q \to 0$, the oscillation frequencies of both the ASV-0 and SSV-0 branches approach zero. The positions of the onset frequencies for the higher order branches obey the following sequence: ASV-1, SSV-1, ASV-2, SSV-2, etc. All these branches fall into the sector given by Eq. (23).

It is important to emphasize that the isotropic model failed to predict the behavior of the branch SSV-0 shown in Fig. 2. Indeed, in elastically isotropic media only the ASV-0 mode exists in the limit $Q \to 0$, and the SSV-0 mode is the first excited mode with finite Ω and Q onsets.[5,6,16] For elastically anisotropic media, we found that the modes of both symmetries ASV and SSV can exist at $Q \to 0$. Mathematically, this is because the oscillating and decaying solutions in the B material allow to satisfy the boundary conditions of Eq. (6) for the two lowest modes. These lowest ASV-0 and SSV-0 branches exhibit a relatively small separation. We have studied the SSV-0 branch in detail, particularly for small Q. In Fig. 3(a), the SSV-0 mode with $Q=0.3$ is presented. One can see that this mode represents lattice vibrations in a wide spatial region outside the QW layer. Their magnitude oscillates and decays very slowly.[26]

From the analysis presented in Sec. II, it follows that for each branch the real part of the decay factors $\mathrm{Re}[R_{\mp}(\omega,q)]$ vanishes near the onset and, thus, the confinement of the corresponding solutions is weak. The development of the branch at the higher Q leads to a progressive increase in both the mode confinement and localization of the elastic energy inside the QW. In Figs. 3(b) and 3(c), we present the results of calculations of the displacement vector [Eq. (7)] and the elastic energy [Eq. (18)] at $Q=2$ for the SSV-0 branch. One can see that the lattice vibrations are well confined inside the QW layer.

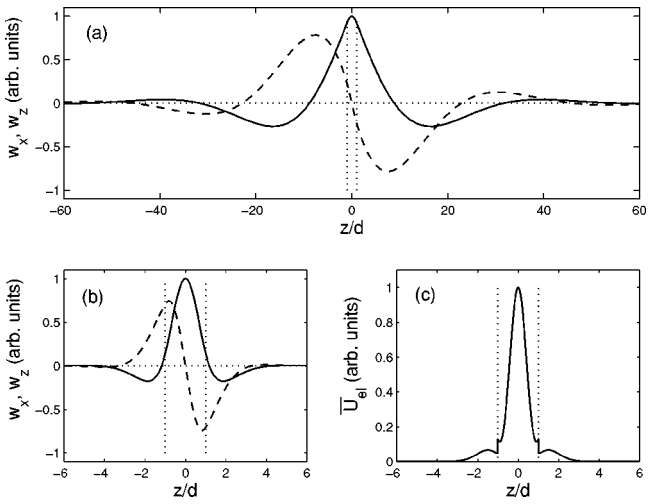

FIG. 3. (a) and (b) Spatial distribution of the displacement fields, and (c) elastic energy for the SSV-0 phonons in Si/Ge/Si QW heterostructures. Q is fixed at 0.3 for (a) and 2.0 for (b) and (c). Vertical dotted lines indicate the heterointerfaces. Distributions $w_x(z)$ and $w_z(z)$ are shown by solid and dashed lines, respectively [(a) and (b)].

Generally, the lattice vibrations of the SV modes correspond to quite complex motions of the media. Figure 4 illustrates the displacement vector fields for both the ASV-0 and SSV-0 modes computed at a fixed moment of time with the same dimensionless wave vector $Q=2$. The patterns along the x axis correspond to the dimensionless wave period $2\pi/Q$. The figure illustrates the difference in the displacement patterns of waves of different symmetries. These data straightforwardly demonstrate that SV waves comprise both longitudinal and transverse displacements.

The lowest SV modes for $Si/Si_{0.5}Ge_{0.5}/Si$ QW heterostructures are presented in Fig. 5(a). They behave quite similar to the modes of the previous case. Due to a lower elastic mismatch between Si and $Si_{0.5}Ge_{0.5}$, however, this system

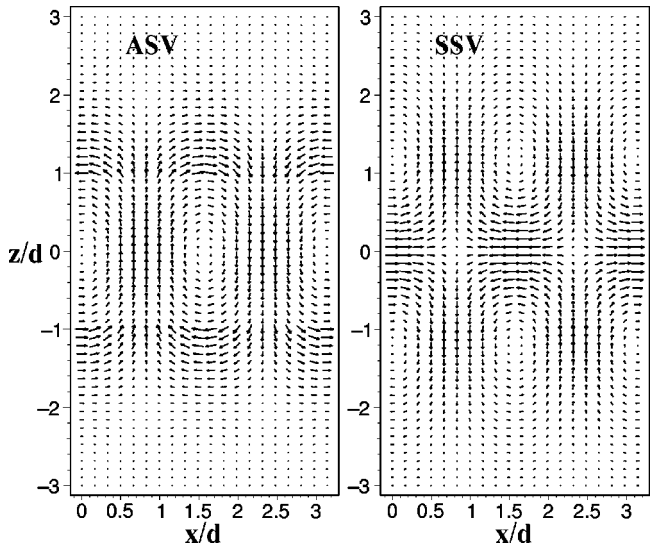

FIG. 4. Displacement vector fields in Si/Ge/Si for SSV-0 and ASV-0 confined modes with $Q=2$.

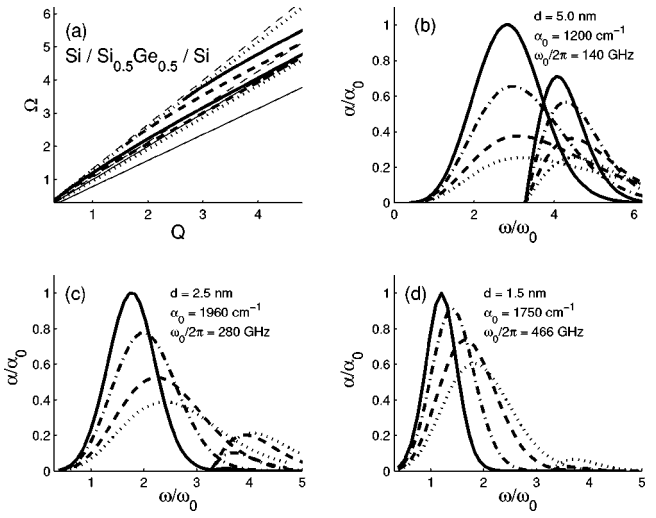

FIG. 5. (a) Dispersion for $Si/Si_{0.5}Ge_{0.5}/Si$ QW heterostructures; notations are the same as in Fig. 2. (b)–(d) Amplification coefficient as a function of phonon frequency at $T=50$ K (solid lines), 100 K (dash-dotted lines), 200 K (dashed lines), and 300 K (dotted lines).

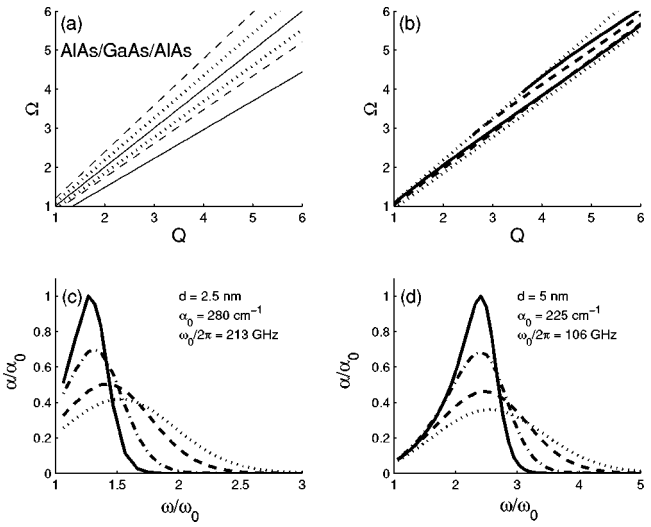

FIG. 6. (a) Overlap of the sectors S_T^M, (b) dispersion of the lowest confined phonon modes, and (c) amplification coefficient $\alpha(\omega)$ in AlAs/GaAs/AlAs QW heterostructures. In (a), sector S_T^B is delimited by thin dashed lines: the upper line has a slope $V_T^{[100],B}$, and the lower line has a slope $V_T^{[101],B}$ sector S_T^A is delimited by thin solid lines: the upper line has a slope $V_T^{[100],A}$, the lower line has a slope $V_T^{[101],A}$, the upper dotted line has a slope V_c^B, and the lower dotted line has a slope V_c^A. The notations of (b) are the same as in Fig. 2, and notations of (c) and (d) are the same as in Figs. 5(b)–5(d).

manifests a narrower sector of Eq. (23) and, consequently, a weaker confinement of the elastic waves.

Summarizing the results of the study of $Si_{1-x}Ge_x$-based QW heterostructures, one can state that for these materials the effect of acoustic-phonon confinement exists in a wide range of alloy composition x. This supports the interpretation of experimental results[10] on the low-dimensional transport in Si/Ge QW's in the temperature interval 0.3–5.5 K. Indeed, the authors of Ref. 10 found that for the QW layers fabricated of Ge and sandwiched between SiGe, the relaxation rate of electron energy directly indicates the reduction of *dimensionality* of the acoustic phonons from 3 to 2. This means that the energy relaxation is due to *two-dimensional (confined)* phonons. On the other hand, for the QW layers fabricated of Si and sandwiched between SiGe materials the phonon dimensionality was found to be 3.

In AlAs/GaAs QW heterostructures, an extreme case of the weak confinement can be observed. As shown in Fig. 6(a), these heterostructures are characterized by an overlap between the sectors S_T^B and S_T^A. It is important to emphasize that for such a case the isotropic elastic model[5,16] cannot predict the existence of confined SV waves because in this model each sector $S_{L,T}^M$ reduces to a line. Instead, criterion (23) resolves the confinement problem even for this case. The dispersion curves for the lowest confined SV modes in an AlAs/GaAs/AlAs QW are shown in Fig. 6(b). The behavior of this dispersion curves is quite similar to that analyzed previously, except for a decrease in the spacing between the SSV-0 and ASV-0 branches, and the larger frequency–wave-vector onsets for the upper branches.

IV. AMPLIFICATION OF CONFINED PHONONS BY ELECTRON DRIFT

Now we shall consider amplification of confined acoustic phonons through the interaction with two-dimensional carriers. Apparently, the electrons localized in a QW are coupled to all existing phonon modes. However, the phonons considered above and two-dimensional electrons are confined into almost the same spatial region and they should manifest the strongest interaction. To analyze the electron-confined phonon interaction, we will assume that only the lowest two-dimensional subband is populated by electrons, and that the energy distances to the next subbands are larger than the energies of the phonons under consideration. The electron wave functions are $\Psi_{l,k}(r,z)=(1/\sqrt{L_xL_y})e^{ikx}\psi(z)$, where k is the two-dimensional electron wave vector, and L_y and L_x are the lateral dimensions of the sample. In making estimates, we assume that the barriers confining the electrons are infinitely high and $\psi(z)=\cos(\pi z/2d)/\sqrt{d}$. The energy of the electrons populating the lowest subband is $E(k)=\hbar^2k^2/2m^*$, where m^* is the effective mass. The electron motion along the QW layer is supposed to be semiclassical, and is described by a distribution function $F[k_x,k_y]$ dependent on the applied electric field. Then we suppose the deformation potential mechanism for electron-phonon coupling with the interaction energy $b\,\mathrm{div}(\mathbf{u})$; b is the deformation potential constant.

A quantum-mechanical description of carrier interaction with a given $\{\nu,q\}$-phonon mode leads to the development of the kinetic equation for the mode population. Such an analysis was made in Ref. 16. When the population of the mode becomes large and the phonon subsystem can be treated semiclassically, we can introduce the intensity of the corresponding acoustic wave and define the amplification (absorption) coefficient, $\alpha_{\nu q}$. This coefficient describes the rate of increase (decrease) in the acoustic wave intensity per unit length. Under the above assumption, we have obtained

the following formula for the amplification coefficient of the confined $\{\nu,q\}$ wave:[16]

$$\alpha_{\nu q}=\frac{m^*}{\pi\hbar^3|q|}\frac{|\mathcal{M}(q)|^2}{[\kappa^{(el)}(q)]^2\left|\frac{d\omega_{\nu,q}}{dq}\right|}L_xL_y[\mathcal{I}_\nu^{(+)}(q)-\mathcal{I}_\nu^{(-)}(q)]. \tag{24}$$

Here

$$\mathcal{M}(q)\equiv ib\int_{-\infty}^{\infty}\left(qw_{\nu q,x}(z)+\frac{dw_{\nu q,z}(z)}{dz}\right)\psi^2(z)dz$$

is the matrix element of the electron-phonon interaction. $\kappa^{(el)}(q)$ is the electron permittivity defined as

$$\kappa^{(el)}(q)=1+\frac{2\pi e^2 d}{\kappa}\mathcal{A}(q)\mathcal{B}(qd), \tag{25}$$

where κ is the dielectric constant, and the polarization operator $\mathcal{A}(q)$ and the function $\mathcal{B}$ are in the forms

$$\mathcal{A}(q)=-\frac{2}{L_xL_y}\sum_{\mathbf{k}}\frac{F(\mathbf{k})-F(\mathbf{k}-\vec{q})}{E(\mathbf{k})-E(\mathbf{k}-\mathbf{q})},$$

$$\mathcal{B}(s)=\frac{d^2}{s}\int\int_{-\infty}^{\infty}d\zeta d\zeta'\psi^2(\zeta d)\psi^2(\zeta' d)e^{-s|\zeta-\zeta'|}.$$

The population factors $\mathcal{I}_\nu^{(\pm)}$ account for the number of electrons interacting with the $\{\nu,q\}$-mode, and are calculated via the electron distribution function

$$\mathcal{I}_\nu^{(\pm)}(\mathbf{q})=\int_{-\infty}^{\infty}dk_yF\left[\mathrm{sgn}(q)\frac{m^*\omega_{\nu q}}{\hbar|q|}\pm\frac{1}{2}q,k_y\right], \tag{26}$$

with $\mathrm{sgn}(x)=1$ for $x>0$ and $\mathrm{sgn}(x)=-1$ for $x<0$.

Depending on the shape of the distribution function $F(k_x,k_y)$, the value $\alpha_{\nu q}$ can be either positive or negative. For the electrons drifting in an applied electric field along the QW layer, the distribution function can be described in terms of a shifted Fermi distribution: $F[k_x,k_y]=F_F[k_x-V_{dr}m^*/\hbar,k_y]$, where $F_F(\mathbf{k})$ is the Fermi function and V_{dr} is the electron drift velocity. In such an approach, Eqs. (24)–(26) express the amplification coefficient as a function of two electron parameters: the electron temperature T and the drift velocity V_{dr}. For a particular heterostructure, a given lattice temperature, and a given applied electric field, both T and V_{dr} can be calculated from the energy and momentum balance equations.[27]

From Eqs. (24)–(26), it follows that for phonons propagating along the electron flux, the amplification coefficient $\alpha_{\nu q}>0$ if the electron drift velocity exceeds the confined-phonon phase velocity: $V_{dr}>\omega_{\nu q}/|q|$. This criterion is, in fact, the well-known condition of the Čerenkov generation effect.[28] If the amplification coefficient caused by the electron-phonon interaction is positive and exceeds all phonon losses, the intensity of the corresponding confined wave(s) should increase exponentially with the coordinate, i.e., we obtain the effect of phonon amplification.

Now we shall return to particular QW heterostructures. For the case of SiGe-based structures, we will focus on *p*-doped QW's. Holes are confined more than electrons in these QW's. In such a case, the lowest subband is heavy-hole-like. The effective mass for the heavy holes in the Si/Ge/Si QW can be estimated as $m^*=0.4m_0$, where m_0 is the free-electron mass. Other parameters are taken from Ref. 21. For an AlAs/GaAs/AlAs QW, we consider phonon interaction with electrons of effective mass $m^*=0.067m_0$.

To compute the amplification coefficient of Eq. (24), we take the concentrations of the carriers and drift velocity to be 10^{12} cm^{-2} and 2.5 V_T^A, respectively. In the case of Si/Ge/Si heterostructure, for instance, $V_{dr}=2.5$ V_T^A corresponds to 9×10^5 cm/s and can be reached in modest electric fields.[6] As follows from Table I and Figs. 2, 5(a), and 6(b), the chosen value of V_{dr} ensures the fulfillment of the Čerenkov criterion for any branch of the confined acoustic modes in all systems considered in this paper.

First we consider a 100-Å $Si/Si_{0.5}Ge_{0.5}/Si$ heterostructure. The amplification coefficient for this case is presented in Fig. 5(b) as a function of the dimensionless phonon frequency ω/ω_0 for SSV-0 and SSV-1 phonon branches. Calculations are performed for different temperatures: $T=50$, 100, 200, and 300 K. One can see that a considerable amplification effect exists for both phonon branches. The basic behavior of α is similar to that found in the isotropic model calculations presented in Ref. 16. The maximum amplification is achieved at low temperatures: $\alpha_{SSV-0}(364\text{ GHz},\ 50\text{ K})=1200$ cm^{-1}. As the temperature increases above 50 K, the amplification coefficient decreases. Nevertheless, it remains high even at $T=300$ K (about 300 cm^{-1} at the peak). Note that the amplification of the phonon modes belonging to the second branch starts at a finite frequency which coincides with the onset of the SSV-1 dispersion.

In general, the magnitude of amplification depends on three factors: carrier population factor, the degree of wave localization, and the relative magnitude of longitudinal-like vibrations in the confined wave. All these factors can be changed by a variation of the materials composing the QW, doping type, concentration, and temperature, as well as by the width of the well. The influence of the latter parameter is illustrated in Figs. 5(c) and 5(d). The reduction of d for the same $Si/Si_{0.5}Ge_{0.5}/Si$ system leads to an increase in the magnitude of amplification for the first amplification band, as well as to the inversion of the temperature dependence of the amplification magnitudes and their suppression for the second amplification band. The frequency which corresponds to the maximum of amplification also tends to increase for higher temperatures.

The magnitude of the amplification essentially depends not only on the degree of phonon confinement, but also on the value of m^*. From this point of view, it is hard to expect that amplification of the phonons by electrons in an AlAs/GaAs/AlAs QW will lead to a large effect. Nevertheless, as indicated by the data presented in Figs. 6(c) and 6(d), the low-temperature amplification of the phonons with a frequency of about 200 GHz can reach hundreds of cm^{-1} even in this heterostructure. The second amplification band is completely suppressed.

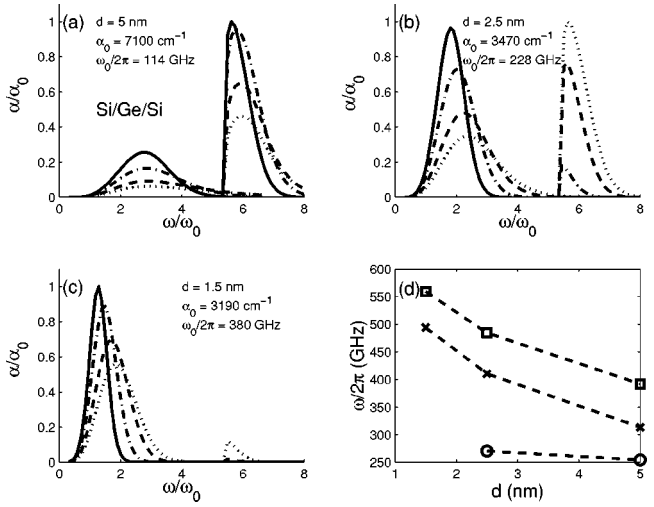

FIG. 7. (a)–(c) Amplification coefficient in Si/Ge/Si heterostructures as a function of phonon frequency at $T=50$ K (solid lines), 100 K (dash-dotted lines), 200 K (dashed lines), and 300 K (dotted lines). (d) Confined phonon frequencies at the maxima of amplification coefficients presented in Figs. 5(b)–5(d), 6(c), and 6(d), and 7(a)–7(c) for SSV-0 phonon branches.

A significant increase in the amplification coefficient can be achieved for Si/Ge/Si QW heterostructures, where the phonon confinement is stronger due to the larger elastic mismatch in the layers composing the structures. Moreover, these structures manifest a unique dependence of α on the width of the well and temperature. As shown in Fig. 7(a), a 100-Å Si/Ge/Si QW is expected to have a broad SSV-0 amplification band and a relatively narrow SSV-1 amplification band. Unlike all previously considered cases, the strongest amplification with a record value of 7100 cm^{-1} is expected for the second band at the frequency of 640 GHz. Additionally, this value remains almost independent on temperature in the interval $T=50$–100 K. A reduction of the well width to 50 Å leads to another interesting effect. Figure 7(b) shows that in this case both bands can manifest strong and almost equal amplifications so that α can reach its maximum for the first band at low temperature whereas almost the same value of α can be achieved at high temperature for the band SSV-1. Note that both the SSV-0 ($T=50$ K) and SSV-1 ($T=300$ K) bands are relatively narrow. One can see that the magnitude of the $\alpha_{SSV-1}(300\ \mathrm{K})$ is almost insensitive to the variation of d from 50 to 25 Å. At $d=15$ Å, however, the second band is almost totally suppressed, as shown in Fig. 7(c). Nevertheless, the magnitude of the SSV-0 band amplification remains higher than in the case of the Si/SiGe structure.

For all the structures and amplification bands considered in this paper, the maximum of α shifts toward higher frequencies with increasing temperature. Figure 7(d) shows that the frequency of the amplification maximum also tends to increase when the width of the QW decreases. For the same set of widths, the latter effect is less pronounced in AlAs/GaAs/AlAs heterostructures where the sector with the confined phonon dispersion branches restricted in the (ω,q) plane by Eq. (23) is narrow. This leads to a relatively small carrier-phonon interaction: the phonons with phase velocities close to V_c^B are weakly confined, whereas for the phonons with phase velocities close to V_c^A the contribution of the longitudinal-like vibrations to the SV mode vanishes. As a result, the maximum amplification can be reached in a relatively narrow interval of phonon frequencies and wave vectors, so that the dependence of the properties of the electron-phonon system on d has only a minor impact on the position of the maximum. This explanation is also supported by the other results presented in Fig. 7(d). One can see that for SiGe-based structures, a tendency—the wider the sector defined by Eq. (23), the more sensitive the position of the maximum becomes to the well width—is manifested.

Note that although the dependence presented in Fig. 7(d) for the Si/Ge/Si structure is stronger than that for the $Si/Si_{0.5}Ge_{0.5}/Si$ system, the absolute values of frequencies which correspond to the maxima of α are smaller. This occurs as a result of a faster development of the carrier-phonon interaction upon increasing q or ω in the Si/Ge/Si QW, where for a mode with the same degree of confinement the relative contribution of the longitudinal vibrations is higher.

In efforts to realize the large amplification of confined phonons by electron drift at high frequencies, it is important to keep in mind that an increase in the phonon frequency gives rise to an enlargement of phonon losses due to crystal anharmonicity, scattering on defects, etc. For frequencies less than 1 THz, phonon losses due to the anharmonicity and scattering by natural defects (isotopes) are well below the phonon gain estimated for heterostructures considered in this study.[29] To observe the amplification effect, however, one should use well-designed and high-quality QW heterostructures.

V. SUMMARY

We have performed an analysis of confined acoustic vibrations in QW heterostructures composed of cubic materials. A general criterion of the occurrence of confined phonons in such structures has been derived. We have presented a realistic analysis of these phonons in cubic Si/Ge/Si, $Si/Si_{0.5}Ge_{0.5}/Si$ and AlAs/GaAs/AlAs QW heterostructures with a focus on shear-vertical vibrations. We have found that the model of an elastically isotropic media cannot be applied to layered systems composed of materials with relatively small elastic mismatch and negative anisotropy factor. AlAs/GaAs/AlAs QW heterostructures belong to this class of systems. We have calculated dispersion curves for the confined phonons. For all of the analyzed structures, we have shown that the behavior of the lowest phonon branches is quite different from that in the model of elastically isotropic media. We have studied the displacement fields corresponding to these phonons, and discovered their complex internal structure. In the subterahertz and terahertz frequency range, SV phonons are strongly confined inside the QW layers. These results support the experimental observation[10] of the reduction of the dimensionality of acoustic phonons efficiently coupled to the two-dimensional holes in Si/Ge/Si quantum wells.[30]

For p-doped $Si/Si_xGe_{1-x}/Si$ and n-doped AlAs/GaAs/

AlAs quantum-well heterostructures, we have studied the effect of amplification of the confined phonons by the drift of low-dimensional carriers. We have shown that the amplification coefficient can be of the order of hundreds of cm^{-1} for $Al_xGa_{1-x}As$ heterostructures, and of the order of thousands of cm^{-1} for SiGe heterostructures in the terahertz phonon frequency range. This suggests that electric methods for the amplification and generation of terahertz coherent phonons can be realized in these technologically important QW heterostructures.

ACKNOWLEDGMENTS

This work was supported by the Air Force Office of Scientific Research and the U.S. Army Research Office. V.A.K. would like to acknowledge the support from CRDF Project #UE2-2439-KV-02.

APPENDIX A

The characteristic matrix for SSV waves $\mathcal{D}^{SSV}$ is

$$\mathcal{D}_{11}=\cosh(\mathcal{R}_- d), \quad \mathcal{D}_{12}=\cosh(\mathcal{R}_+ d),$$

$$\mathcal{D}_{13}=\cos(\mathcal{R}_i d), \quad \mathcal{D}_{14}=\sin(\mathcal{R}_i d),$$

$$\mathcal{D}_{21}=\xi_A R_- \chi_- \sinh(\mathcal{R}_- d), \quad \mathcal{D}_{22}=\xi_A R_- \chi_- \sinh(\mathcal{R}_- d),$$

$$\mathcal{D}_{23}=\xi_B[\zeta_1\cos(\mathcal{R}_i d)-\zeta_2\sin(\mathcal{R}_i d)],$$

$$\mathcal{D}_{24}=\xi_B[\zeta_2\cos(\mathcal{R}_i d)+\zeta_1\sin(\mathcal{R}_i d)],$$

$$\mathcal{D}_{31}=(1-\xi_A\chi_-)R_-\sinh(\mathcal{R}_- d),$$

$$\mathcal{D}_{32}=(1-\xi_A\chi_+)R_+\sinh(\mathcal{R}_+ d),$$

$$\mathcal{D}_{33}=[\{\zeta_2\sin(\mathcal{R}_i d)-\zeta_1\cos(\mathcal{R}_i d)\}\xi_B-R_i\sin(\mathcal{R}_i d) - R_r\cos(\mathcal{R}_i d)]C_{44}^B/C_{44}^A,$$

$$\mathcal{D}_{34}=[-\{\zeta_1\sin(\mathcal{R}_i d)+\zeta_2\cos(\mathcal{R}_i d)\}\xi_B+R_i\cos(\mathcal{R}_i d) - R_r\sin(\mathcal{R}_i d)]C_{44}^B/C_{44}^A,$$

$$\mathcal{D}_{41}=\left[\frac{C_{11}^A}{C_{12}^A}\xi_A R_-^2\chi_- +1\right]\cosh(\mathcal{R}_- d),$$

$$\mathcal{D}_{42}=\left[\frac{C_{11}^A}{C_{12}^A}\xi_A R_+^2\chi_+ +1\right]\cosh(\mathcal{R}_+ d),$$

$$\mathcal{D}_{43}=\frac{C_{11}^B}{C_{12}^A}\xi_B[(\chi_r\zeta_3-2R_rR_i\chi_i)\cos(\mathcal{R}_i d) + (\chi_i\zeta_3+2R_rR_i\chi_r)\sin(\mathcal{R}_i d)]+\frac{C_{12}^B}{C_{12}^A}\cos(\mathcal{R}_i d),$$

$$\mathcal{D}_{44}=\frac{C_{11}^B}{C_{12}^A}\xi_B[(\chi_r\zeta_3-2R_rR_i\chi_i)\sin(\mathcal{R}_i d) - (\chi_i\zeta_3+2R_rR_i\chi_r)\cos(\mathcal{R}_i d)]+\frac{C_{12}^B}{C_{12}^A}\sin(\mathcal{R}_i d).$$

The index $A(B)$ denotes the material of the QW (surrounding material); the other notations are

$$\mathcal{R}_\mp \equiv \mathcal{R}_\mp^A,$$

$$\xi_M=\left(\left[C_{11}^M-C_{44}^M+D^M\right]\left[1-\frac{\rho_M}{C_{44}^M}\frac{\omega^2}{q^2}\right]\right)^{-1}, \quad \chi_\mp \equiv \chi_\mp^A \text{ with}$$

$$\chi_\mp^M \equiv C_{11}^M\left[R_{\mp,M}+\frac{[C_{11}^M-C_{44}^M+D^M]^2}{C_{11}^M C_{44}^M}-\left(\frac{C_{11}^M}{C_{44}^M}-\frac{\rho_M}{C_{44}^M}\frac{\omega^2}{q^2}\right)\right],$$

$(R,\chi)_r \equiv |\mathrm{Re}[(R,\chi)_\mp^B]|$, $(R,\chi)_i \equiv |\mathrm{Im}[(R,\chi)_\mp^B]|$, $\zeta_1 \equiv \chi_i R_i - \chi_r R_r$, $\zeta_2 \equiv \chi_i R_r + \chi_r R_i$, and $\zeta_3 \equiv R_r^2 - R_i^2$. The matrix $\mathcal{D}^{ASV}$ can be obtained from $\mathcal{D}^{SSV}$ by making the following substitutions in the first two columns: sin→cos, sinh →cosh, cos→sin, and cosh→sinh.

APPENDIX B

In Eq. (20), the characteristic velocities are

$$V_0^2=\frac{2}{\rho(C_{11}+C_{44})}\left(C_{11}C_{44}+D\left\{C_{11}-C_{44}-\frac{D}{2}\right\}\right), \tag{B1}$$

$$V_\mp^2=\frac{2(C_{11}+C_{44})}{\rho(C_{11}-C_{44})^2}\left[\frac{C_{11}-C_{44}-D}{C_{11}+C_{44}} \times\sqrt{2C_{11}C_{44}D\left(\frac{D}{2}+C_{44}-C_{11}\right)} \mp D\left\{\frac{D}{2}+C_{44}-C_{11}\right\}\right]. \tag{B2}$$

[1] A. A. Maradudin, in *Nonequilibrium Phonon Dynamics*, edited by W. E. Bron (Plenum, New York, 1985), p. 395.

[2] F. R. Rollins, T. C. Lim, and G. W. Farnell, Appl. Phys. Lett. **12**, 236 (1968); N. F. Naumenko, J. Appl. Phys. **79**, 8936 (1996); N. F. Naumenko and I. S. Didenko, Appl. Phys. Lett. **75**, 3029 (1999); A. N. Darinskii and M. Welhnacht, J. Appl. Phys. **88**, 471 (2000).

[3] R. Stonely, Proc. R. Soc. London, Ser. A **106**, 416 (1924).

[4] I. V. Ponomarev and A. L. Efros, Phys. Rev. B **63**, 165305 (2001).

[5] L. Wendler and V. G. Grigoryan, Surf. Sci. **206**, 203 (1988); V. G. Grigorian and L. Wendler, Fiz. Tverd. Tela (Leningrad) **33**, 2120 (1991) [Sov. Phys. Solid State **33**, 1193 (1991)].

[6] V. V. Mitin, V. A. Kochelap, and M. Stroscio, *Quantum Heterostructures for Microelectronics and Optoelectronics* (Cambridge University Press, New York, 1999).
[7] M. A. Stroscio, G. J. Iafrate, H. O. Everitt, K. W. Kim, Y. Sirenko, S. Yu, M. A. Littlejohn, and M. Dutta, in *Properties of III-V Quantum Wells and Superlattices*, edited by P. Bhattacharya (Peter Peregrinus Ltd./IEE, London, 1996), p. 194.
[8] G. P. Srivastava, *The Physics of Phonons* (Hilger, Bristol, 1990).
[9] P. Y. Yu and M. Cardona, *Fundamentals of Semiconductors* (Springer-Verlag, Berlin, 1995).
[10] S. H. Song, W. Pan, D. C. Tsui, Y. H. Xie, and D. Monroe, Appl. Phys. Lett. **70**, 3422 (1997).
[11] V. I. Pipa, B. A. Glavin, V. V. Mitin, and M. A. Stroscio, Semicond. Sci. Technol. **13**, A97 (1998).
[12] V. I. Pipa, N. Z. Vagidov, V. V. Mitin, and M. A. Stroscio, Physica B **270**, 280 (1999); Superlattices Microstruct. **27**, 425 (2000).
[13] M. A. Zudov, I. V. Ponomarev, A. L. Efros, R. R. Du, J. A. Simmons, and J. L. Reno, Phys. Rev. Lett. **86**, 3614 (2001).
[14] M. Rotter, A. V. Kalameitsev, A. O. Govorov, W. Ruile, and A. Wixforth, Phys. Rev. Lett. **82**, 2171 (1999).
[15] A. Pinczuk, B. S. Dennis, L. N. Pfeiffer, and K. West, Phys. Rev. Lett. **70**, 3983 (1993); V. I. Talyanskii, J. M. Shilton, M. Pepper, C. G. Smith, C. J. B. Ford, E. H. Linfield, D. A. Ritchie, and G. A. C. Jones, Phys. Rev. B **56**, 15 180 (1997).
[16] S. M. Komirenko, K. W. Kim, A. A. Demidenko, V. A. Kochelap, and M. A. Stroscio, Appl. Phys. Lett. **76**, 1869 (2000); Phys. Rev. B **62**, 7459 (2000).
[17] G. W. Farnell and E. L. Adler, in *Physical Acoustics*, edited by W. P. Mason and R. N. Thurston (Academic, New York, 1972), Vol. IX.
[18] G. W. Farnell, in *Acoustic Surface Waves*, edited by A. A. Oliner (Springer, Heidelberg, 1978).
[19] O. Hardouin-Duparc, E. Sanz-Velasco, and V. R. Velasco, Phys. Rev. B **30**, 2042 (1984).
[20] L. D. Landau and E. M. Lifschitz, *Theory of Elasticity* (Pergamon, Oxford, 1986).
[21] O. Madelung, *Semiconductors. Group IV and III-V Compounds* (Springer, Berlin, 1991).
[22] To calculate the stiffness constants C_{ij}, for $Si_{1-x}Ge_x$ layers, we apply the following linear approximations: $C_{ij,SiGe}=(1-x)C_{ij,Si}+xC_{ij,Ge}$ and $\rho_{SiGe}=(1-x)\rho_{Si}+x\rho_{Ge}$.
[23] S. Adachi, J. Appl. Phys. **58**, R1 (1985).
[24] The solutions $\mathbf{u}_{\nu q}$ are presented in the complex form. Computing Eq. (17) one needs to use $\mathrm{Re}[\mathbf{u}_{\nu q}]$.
[25] Our analysis is based on the assumption that the layers composing a heterostructure are made of materials with cubic symmetry. In structures like $Si/Si_{1-x}Ge_x$, strain lowers the crystal symmetry. However, since the lattice mismatch is relatively small (less than 4%), the elastic theory can still be successfully applied to describe these structures. Taking this into account, we have neglected the strain-induced changes in the elastic moduli.
[26] In the limit $qd \ll 1$, the ASV-0 and SSV-0 branches correspond to weakly localized acoustic waves obtained in the model of the so-called elastic ''flat'' defect studied by A. M. Kosevich and V. I. Khokhlov, Fiz. Tverd. Tela (Leningrad) **10**, 56 (1968) [Sov. Phys. Solid State **10**, 39 (1968)].
[27] D. K. Ferry, *Semiconductors* (MacMillan, New York, 1991).
[28] J. H. McFee, in *Physical Acoustic*, edited by W. P. Masson (Academic, New York, 1966), Vol. IV, p. 1.
[29] S. Tamura, Phys. Rev. B **30**, 849 (1984); **31**, 2574 (1985).
[30] A study of the confined phonon effects on the electron transport is beyond the scope of this paper. Here we only mention that for the established sequence of the confined branches ASV-0, SSV-0, ASV-1, SSV-1, etc., it is important that both lowest branches have zero frequency-onset at $q \to 0$. Indeed, at low temperatures ($k_B T < \hbar\omega^0_{SSV\text{-}1}$, where $\omega^0_{SSV\text{-}1}$ is the onset of the SSV-1 branches), only SSV-0 phonons lead to *intrasubband* scattering and contribute to the resistance.